

Alternative similarity renormalization group generators in nuclear structure calculations

Nuiok M. Dicaire,^{1,2,*} Conor Omand,^{3,2,†} and Petr Navrátil^{2,‡}

¹*Department of Physics, University of Ottawa, Ottawa, ON, K1N 6N5, Canada*

²*TRIUMF, 4004 Wesbrook Mall, Vancouver, BC, V6T 2A3, Canada*

³*Department of Physics and Astronomy, University of British Columbia, Vancouver, BC, V6T 1Z4, Canada*

The similarity renormalization group (SRG) has been successfully applied to soften interactions for *ab initio* nuclear calculations. In almost all practical applications in nuclear physics, an SRG generator with the kinetic energy operator is used. With this choice, a fast convergence of many-body calculations can be achieved, but at the same time substantial three-body interactions are induced even if one starts from a purely two-nucleon (NN) Hamiltonian. Three-nucleon ($3N$) interactions can be handled by modern many-body methods. However, it has been observed that when including initial chiral $3N$ forces in the Hamiltonian, the SRG transformations induce a non-negligible four-nucleon interaction that cannot be currently included in the calculations for technical reasons. Consequently, it is essential to investigate alternative SRG generators that might suppress the induction of many-body forces while at the same time might preserve the good convergence. In this work we test two alternative generators with operators of block structure in the harmonic oscillator basis. In the no-core shell model calculations for ${}^3\text{H}$, ${}^4\text{He}$ and ${}^6\text{Li}$ with chiral NN force, we demonstrate that their performances appear quite promising.

PACS numbers: 21.60.De,21.30.Fe,27.10.+h,27.20.+n

I. INTRODUCTION

One of the major goals of nuclear physics is to understand the structure and dynamics of nuclei, i.e. quantum many-body systems exhibiting bound states, unbound resonances, and scattering states, all of which can be strongly coupled. *Ab initio* (i.e., from first principles) approaches attempt to achieve such a goal starting from accurate basic interactions among nucleons. The modern theory of nuclear forces based on the chiral effective field theory (χEFT) [1, 2] offers a link to the underlying theory of quantum chromodynamics at low energies. Nucleon-nucleon (NN) and three-nucleon ($3N$) interactions derived with the help of the chiral EFT have been recently used with a significant success as input to various many-body techniques. Methods such as the no-core shell model (NCSM) [3, 4], coupled cluster (CC) theory [5, 6], self-consistent Green's functions (SCGF) [7], and in-medium SRG [8] calculate binding energies, excitation energies, separation energies, radii, transition rates, and other observables for light as well as medium mass nuclei. They provide tests of these forces and at the same time provide predictions that can be confronted with experiments. Some of these methods can also be extended to describe resonances, scattering states and even nuclear reactions, e.g., no-core shell model with continuum (NCSMC) [9, 10] or CC with the Gamow basis [11].

Even though the chiral interactions are in general softer than the traditional NN potentials constructed

from the meson-exchange theory, they still pose convergence problems for the many-body methods. Only CC calculations for closed shell nuclei were performed to convergence using bare chiral NN potentials [12, 13]. None of the above many-body methods, however, is at present capable of reaching sufficiently large model spaces when the chiral NN interaction is supplemented by the chiral $3N$ interaction. Consequently, techniques such as the similarity renormalization group (SRG) have been applied to soften the chiral interactions [14–17]. The SRG uses continuous series of unitary transformations of the free-space Hamiltonian H ($H \equiv H_{s=0}$),

$$H_s = U_s H U_s^\dagger, \quad (1)$$

to decouple high-momentum and low-momentum physics. The label s is a flow parameter running from zero toward ∞ , which keeps track of the sequence of Hamiltonians. These transformations are implemented as a flow equation in s

$$\frac{dH_s}{ds} = [\eta_s, H_s] = [[G_s, H_s], H_s], \quad (2)$$

whose form guarantees that the H_s 's are unitarily equivalent [15, 18, 19]. Here, $\eta_s = \frac{dU}{ds}U^\dagger$ is an anti-hermitian SRG generator chosen in a form $\eta_s = [G_s, H_s]$ with a hermitian flow operator G_s . The high- and low-momentum decoupling results in general in a faster convergence of many-body calculations. At the same time, the SRG transformation induces many-body forces, i.e., even if the initial $H_{s=0}$ Hamiltonian includes only two-body interactions, the evolved $H_{s>0}$ Hamiltonians will contain many-body interactions, in principle up to A -body for an A -nucleon system.

In *ab initio* nuclear calculations, the SRG generator has been typically chosen by setting $G_s = T_{\text{rel}}$, where the

*E-mail: ndica015@uottawa.ca

†E-mail: comand92@hotmail.com

‡E-mail: navratil@triumf.ca

T_{rel} is the relative kinetic energy operator [16, 17]. With this choice, the convergence is fast and the evolution of many-body forces can be consistently performed [18]. By varying the flow parameter s and using it as a gauge of the unitarity of SRG transformations, it has been found that starting from a Hamiltonian with a chiral NN interaction, there are significant induced three-body forces, but the induced four- and higher-body interactions appear negligible [20–22]. As the $3N$ interactions can be handled by modern many-body methods, the SRG transformations of Hamiltonians with chiral NN interactions facilitate the solution of the quantum many-body problem for light and medium mass nuclei. However, it has been observed that when the initial chiral $3N$ forces are present in the Hamiltonian, the SRG transformations induce non-negligible four-nucleon interactions for systems with $A \gtrsim 10$ [22, 23] that cannot be currently included in the calculations for technical reasons. The problem can be circumvented to some extent by a reduction of the cutoff of the initial chiral $3N$ interaction [23], but such a solution is far from satisfactory as, e.g., it limits the parameter space of the chiral forces and the range of applicability of these forces. One might expect that in heavier nuclei higher momenta might become more important than in light systems and therefore higher cutoffs of nuclear forces could be appropriate.

The strength of the induced many-body interactions and the rate of convergence depend on the choice of the SRG generator. Consequently, it is essential to investigate alternative SRG generators to the standard choice of $G_s = T_{\text{rel}}$ that might suppress the induction of many-body forces while at the same time might preserve the good convergence. In this work we test two alternative generators with operators G_s of block structure in the harmonic oscillator (HO) basis. We evolve the chiral NN interaction of Refs. [2, 24] using these novel generators and apply them in NCSM nuclear structure calculations for ${}^3\text{H}$, ${}^4\text{He}$ and ${}^6\text{Li}$. In this initial study, we limit ourselves to the SRG NN -only interactions and demonstrate good convergence properties as well as a reduction of the induced three- and higher many-body forces compared to the standard kinetic-term generator.

In Sect. II, we introduce the tested alternative generators and provide a brief description of the NCSM approach. Our results are summarized in Sect. III. Conclusions and outlook are given in Sect. IV.

II. FORMALISM

A. Background

The starting Hamiltonian of *ab initio* approaches can be written as

$$H = T_{\text{rel}} + \mathcal{V} = \frac{1}{A} \sum_{i < j} \frac{(\vec{p}_i - \vec{p}_j)^2}{2m} + \sum_{i < j}^A V_{\text{NN},ij} + \sum_{i < j < k}^A V_{\text{NNN},ijk}, \quad (3)$$

where m is the nucleon mass, $V_{\text{NN},ij}$ is the NN interaction, and $V_{\text{NNN},ijk}$ is the $3N$ interaction. The $T_{\text{rel}} = \frac{1}{A} \sum_{i < j} \frac{(\vec{p}_i - \vec{p}_j)^2}{2m}$ is the intrinsic kinetic energy of the A -nucleon system. In the present work, we employ the chiral N^3LO NN interaction of Refs. [2, 24] that fits two-nucleon scattering data accurately up to ≈ 300 MeV. We omit the chiral $3N$ interaction in this initial study.

The SRG transformation can be performed systematically starting from the two-nucleon system, then proceeding to the three-nucleon system, etc. Embedding the SRG evolved NN interaction in the three-nucleon space allows isolation of the pure three-nucleon part. Similarly, the SRG evolved two-nucleon and the three-nucleon interaction can be embedded in the four-nucleon space and the SRG evolved four-nucleon part can be isolated, etc., although in practice the procedure has been so far performed only up to the three-nucleon level (note, however, that first attempts to calculate and apply SRG induced four-nucleon interactions have been already done [25]). This procedure is particularly well established for the $G_s = T_{\text{rel}}$ choice of the generator [18].

The SRG evolution of the $A=2$ system is typically performed in the momentum space [16–18, 26]. On the other hand, the SRG evolution of the $A=3$ system has been first accomplished using the HO basis [20, 21] although later a momentum space implementation [27] and also hyperspherical momentum implementation [28] have been achieved.

While the original choice for G_s advocated by Wegner and collaborators [15, 19] and applied extensively in condensed matter is the diagonal component of the Hamiltonian $G_s = H_s^d$, in most practical applications of the SRG in nuclear physics, the $G_s = T_{\text{rel}}$ choice in the generator was used. However, there were several exploratory studies focusing on alternative generator choices. As to the use of the diagonal generator in nuclear physics see Ref. [29]. Then in Ref. [30], a block diagonal operator

$$G_s = \begin{pmatrix} P_\Lambda H_s P_\Lambda & 0 \\ 0 & Q_\Lambda H_s Q_\Lambda \end{pmatrix} \quad (4)$$

in the two-nucleon momentum space was introduced and tested in nucleon-nucleon phase shift calculations. In a partial wave momentum representation, the projection operators P and $Q = 1 - P$ are step functions defined by

a sharp cutoff Λ on relative momenta. With this choice, the SRG evolved NN potential is loosely related to the low momentum interaction $V_{\text{low}k}$ constructed by a renormalization group method by preserving the two-nucleon T matrix [31, 32].

A variation of the standard kinetic operator choice was explored in Ref. [33] where the G_s was chosen as functions of T_{rel} . In particular, $G_s = -\frac{\sigma^2}{1+T_{\text{rel}}/\sigma^2}$ and $G_s = -\sigma^2 e^{-T_{\text{rel}}/\sigma^2}$ were considered with a parameter σ controlling the separation of a low-momentum region. It was demonstrated that with these generators the computational time is reduced and, at the same time, the low- and high-momentum separation can be tailored to some extent by particular choices of σ . However, these generators were only tested in two-nucleon calculations and in few-body calculations in a one-dimensional model, i.e., no realistic nuclear calculations with $A>2$ were performed with these or any other alternative generators.

B. Block SRG generators

We introduce and test in few nucleon calculations two alternative generators with the flow operator G_s of block structure in the HO basis. As most of the *ab initio* many-body methods employ the HO basis in one way or another, it is sensible to consider generators with cuts in the HO basis.

First, let us define an SRG generator with the G_s as the block-diagonal part of H_s in analogy with Eq. (4) but in the HO, rather than the momentum basis, i.e.,

$$G_s^A = \begin{pmatrix} P_{\text{gen}} H_s P_{\text{gen}} & 0 \\ 0 & Q_{\text{gen}} H_s Q_{\text{gen}} \end{pmatrix} \quad (5)$$

$$P_{\text{gen}} : N \leq N_{\text{gen}} \quad Q_{\text{gen}} : N > N_{\text{gen}}$$

with N the number of HO excitations of all nucleons above the minimum configuration in A -nucleon basis states. See the panel (a) of Fig. 1 for a schematic representation. As T_{rel} is band-diagonal in the HO basis and drives the Hamiltonian to be band-diagonal, G_s^A should drive the Hamiltonian to be block-diagonal in the spirit of the Okubo-Lee-Suzuki approach [34–37] used, e.g., in earlier NCSM studies [3]. We let N_{gen} , which determines the size of P_{gen} , be independent of the definition of the A -nucleon basis space defined, e.g., in the NCSM calculations by $N \leq N_{\text{max}}$.

Second, let's consider a generator with the flow operator G_s given by (see Fig. 1, panel (b))

$$G_s^B = T_{\text{rel}} + P_{\text{gen}} V_s P_{\text{gen}}, \quad P_{\text{gen}} : N \leq N_{\text{gen}}. \quad (6)$$

With this choice, a Hamiltonian with a potential with zero matrix elements for basis states with $N > N_{\text{gen}}$ will not be transformed. A realistic potential with this property is, e.g., the inverse-scattering JISP NN interaction [38]. More generally, if a (starting) potential has only weak matrix elements in the basis states with $N > N_{\text{gen}}$,

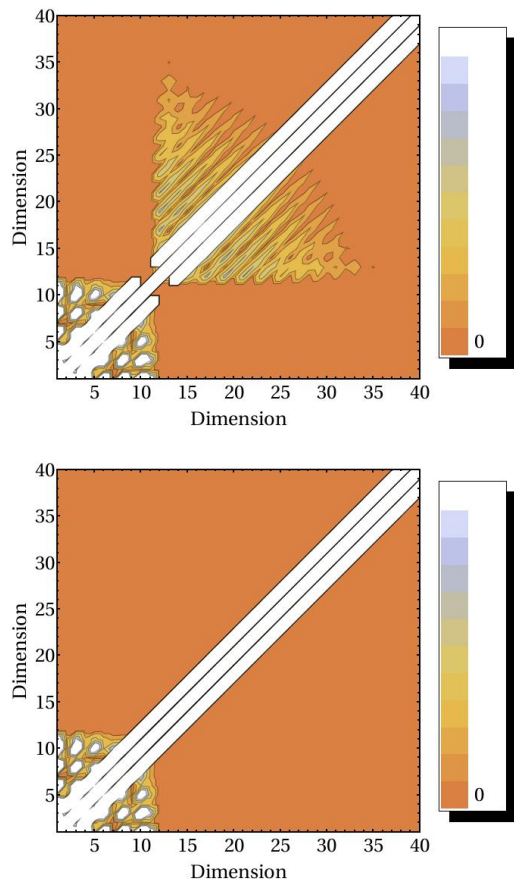


FIG. 1: (color online) Absolute values of matrix elements of the flow operator $G_{s=0}^A$ (top) and $G_{s=0}^B$ (bottom) in the relative-coordinate HO basis of the 3S_1 – 3D_1 NN channel. The $N_{\text{gen}}=10$ was used with the corresponding size of the model space 11. The three white bands along the diagonal correspond to large matrix elements of the kinetic operator. The initial ($s=0$) chiral $N^3\text{LO}$ NN interaction of Refs. [2, 24] was used. The largest matrix elements are shown in white.

it will be only mildly affected by the SRG transformation generated by the flow operator G_s^B . As long as we can reach a basis with, e.g., $N_{\text{max}} \geq N_{\text{gen}}$, we can solve the many-nucleon problem of such a Hamiltonian within, e.g., the NCSMC method [10]. It is then counterproductive to SRG transform such a Hamiltonian using, e.g., the standard $G_s = T_{\text{rel}}$ and generate many-body terms in the process. SRG transformations generated with G_s^B (and also by G_s^A) will in general modify the initial Hamiltonian less than the $G_s = T_{\text{rel}}$ transformations, i.e., one may hope to induce weaker many-body forces. Further, the G_s^B , unlike the G_s^A (5), will not strive to eliminate the strong T_{rel} matrix elements that couple N_{gen} with $N_{\text{gen}}+2$ basis states.

We note that both G_s^A and G_s^B now depend on the HO frequency Ω . Consequently, the evolved Hamiltonian will no longer be variational with respect to Ω . However,

these generators may suppress the induction of three- and higher-body terms, making it easier to preserve the unitarity of the transformation while being computationally easier.

C. NCSM

To test the alternative SRG generators, we perform NCSM calculations for light nuclei. The *ab initio* NCSM is a technique appropriate for the description of bound states or for approximations of narrow resonances. With the Hamiltonian given by Eq. (3), nuclei are considered as systems of A non-relativistic point-like nucleons interacting through realistic inter-nucleon interactions, i.e., those that describe accurately two-nucleon and, possibly, three-nucleon systems. All nucleons are active degrees of freedom. Translational invariance as well as angular momentum and parity of the system under consideration are conserved. The many-body wave function is cast into an expansion over a complete set of antisymmetric A -nucleon HO basis states containing up to N_{\max} HO excitations above the lowest possible configuration:

$$|\Psi_A^{J^\pi T}\rangle = \sum_{N=0}^{N_{\max}} \sum_i c_{Ni} |ANiJ^\pi T\rangle. \quad (7)$$

Here, N denotes the total number of HO excitations of all nucleons above the minimum configuration, $J^\pi T$ are the total angular momentum, parity and isospin, and i additional quantum numbers. The sum over N is restricted by parity to either an even or odd sequence. The basis is further characterized by the frequency Ω of the HO well and may depend on either Jacobi relative or single-particle coordinates. In the former case, the wave function does not contain the center of mass (c.m.) motion, but antisymmetrization is complicated [39]. In the latter case, antisymmetrization is trivially achieved using Slater determinants, but the c.m. degrees of freedom are included in the basis. The HO basis within the N_{\max} truncation is the only possible one that allows an exact factorization of the c.m. motion for the eigenstates, even when working with single-particle coordinates and Slater determinants. Calculations performed with the two alternative coordinate choices are completely equivalent [4].

D. Parameters

To assess the performance of the alternative generators, we perform the SRG transformations in the $A=2$ system using the HO basis (with $N_{\max} \approx 300$ sufficient for convergence). Then we apply the SRG evolved NN interaction in $A>2$ NCSM calculations. The initial chiral $3N$ interaction as well as the SRG induced $3N$ interaction is neglected in this first study. It will be a subject of a future investigation. We compare results obtained

using the block generators with flow operators G_s^A (5) and G_s^B (6) to the standard generator with $G_s=T_{\text{rel}}$.

In our study, we vary the following four parameters:

- N_{gen} : The total number of HO excitations that defines the projector P_{gen} and sets the dimension of the blocks of G_s^A and G_s^B .
- s : (or $\lambda \equiv 1/s^{1/4}$) Sets the degree of SRG evolution (larger s , smaller λ , is more evolved).
- N_{max} : The total number of HO excitations used in the NCSM calculation.
- $\hbar\Omega$: HO basis parameter that controls the shape of the HO potential well and the eigenenergies.

and examine the effects on the Hamiltonian, convergence, and calculated binding energies in ${}^3\text{H}$, ${}^4\text{He}$, and ${}^6\text{Li}$.

III. RESULTS

A. SRG evolved NN potentials

In Fig. 2 we show the evolved NN potentials in the Jacobi coordinate two-nucleon HO basis of the 3S_1 - 3D_1 NN channel. The dimension of the model space P_{gen} is equal to 11, when using generators A and B with $N_{\text{gen}}=10$ in the SRG transformation. The potentials are shown at different degree of the evolution (i.e. different values of the flow parameter s or λ). The evolved potentials depend on the dimension of the model space P_{gen} , which is determined by the parameter N_{gen} , and to some extent also on the HO frequency.

The evolved NN potentials obtained with both generators are similar at high λ (low s). In both cases we see that the potentials are driven to a block-diagonal form as we expected. With generator A, when evolving below $\lambda \sim 1.6 \text{ fm}^{-1}$ the strong coupling at the boundary of the P_{gen} and Q_{gen} spaces due to the kinetic operator induced significant off-diagonal matrix elements and the matrices have a less pronounced block structure. This is attributed to the design of this generator, i.e., to the fact that the large coupling elements of the kinetic operator at the boundary are removed from the flow operator. We do not eliminate these coupling matrix elements when using the generator B. The resulting evolved NN potential in that case has a clearly visible block structure and a narrow diagonal part in the Q_{gen} space.

B. ${}^3\text{H}$ and ${}^4\text{He}$

Figure 3 presents the bare initial and the SRG evolved NN potentials in the antisymmetrized Jacobi-coordinate three-nucleon HO basis for the $J^\pi T = \frac{1}{2}^+ \frac{1}{2}$ ${}^3\text{H}$ channel for various sizes of the three-nucleon model space characterized by N_{max} . In Fig. 4, we show the corresponding ${}^3\text{H}$

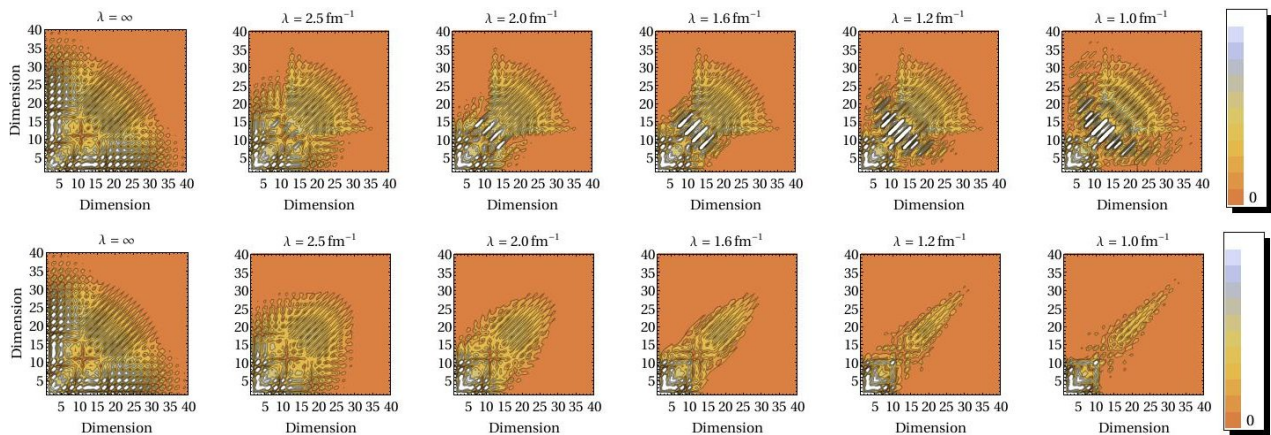


FIG. 2: (color online) Absolute values of the SRG evolved NN potential matrix elements in the relative-coordinate HO basis of the 3S_1 – 3D_1 NN channel for (top row) Generator A and (bottom row) Generator B for various degrees of evolution. The $N_{\text{gen}}=10$ was used with the corresponding size of the model space 11. The initial ($s=0$) chiral $N^3\text{LO}$ NN interaction of Refs. [2, 24] was used.

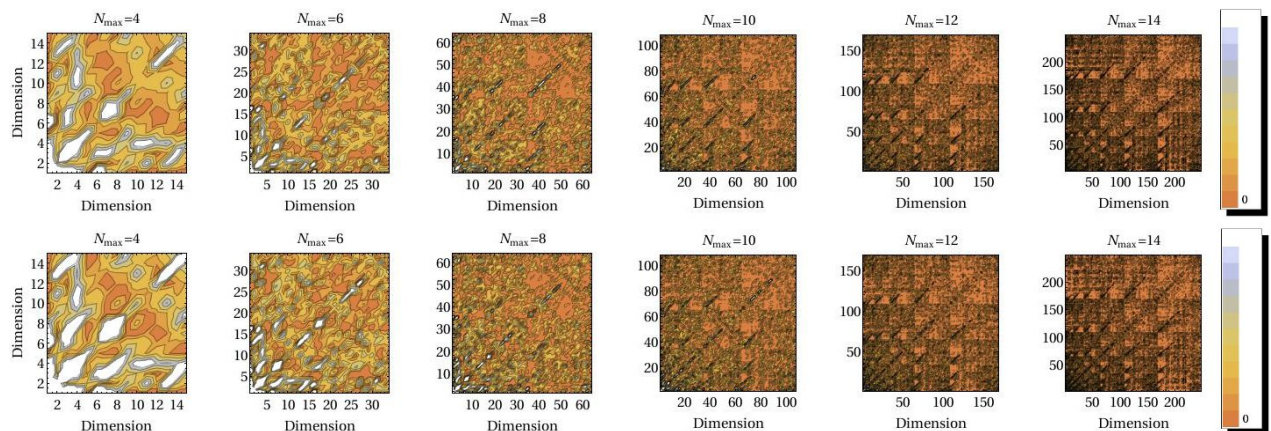


FIG. 3: (color online) Absolute values of the NN potential matrix elements in the antisymmetrized Jacobi-coordinate three-nucleon HO basis for the $J^\pi T = \frac{1}{2}^+ \frac{1}{2}$ ${}^3\text{H}$ channel for various sizes of the three-nucleon model space. Bare initial NN interaction (top row) and the SRG evolved NN interaction with the generator B (bottom row) with $N_{\text{gen}}=10$, HO frequency of $\hbar\Omega=24$ MeV and the SRG flow parameter $\lambda = 2.0$ fm^{-1} were used.

ground-state energy as a function of the parameter N_{max} . A subtle block structure is visible in all plots showing the potential, although clearly not of the type seen in the two-nucleon basis (Fig. 2). Although we do not see significant distinguishable differences due to the SRG evolution, the plots showing the energy as a function of N_{max} clearly give different energies depending on the generator that is used, proving that differences are present in the NN potentials. Fig. 4 demonstrates that convergence is somewhat slower for the generators A and B compared to the standard $G_s=T_{\text{rel}}$, with the converged ground-state energies being much closer to the bare potential result obtained with the bare initial NN potential. Clearly, the convergence is much faster with any of the SRG evolved NN potential compared to the bare one.

Figures 5 (a) and (b) also present ground-state ener-

gies obtained after evolving the NN potentials with SRG transformations. In particular, Figure 5 (a) examines the energy dependence as a function of the basis dimension, N_{max} , for ${}^3\text{H}$ while Figure 5 (b) presents the same results for ${}^4\text{He}$. We show the curves obtained for the two block structured generators. In order to characterize these new generators we also include as a mean of reference the ground-state energies obtained by the bare initial interaction and the ones obtained by using the kinetic term $G_s=T_{\text{rel}}$ as the flow operator for the SRG evolution. The frequency is set to 24 MeV and the evolution is performed up to $\lambda = 2.0$ fm^{-1} . The values obtained with the kinetic term, $G_s=T_{\text{rel}}$, as the flow operator show the largest binding energy for both ${}^3\text{H}$ and ${}^4\text{He}$, and are farther away from the values obtained for the bare interaction than any of the values obtained with generator A or B. Never-

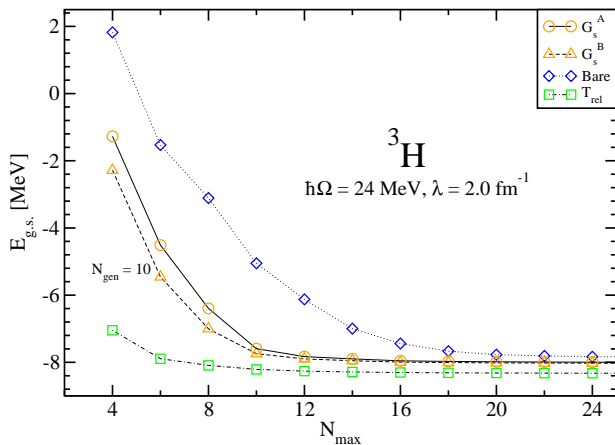


FIG. 4: (color online) The ${}^3\text{H}$ ground-state energy dependence on the size of the basis using the SRG evolved NN potentials presented in Fig. 3. For a comparison, calculations with the (bare) initial chiral $N^3\text{LO}$ NN interaction and with the SRG evolved NN using the $G_s=T_{\text{rel}}$ flow operator are also shown.

theless, this generator gives an extremely quick convergence, which makes it, to this day, the most widely used generator when SRG techniques are employed in nuclear physics. We seek to examine the convergence properties of the two generators proposed in this study, as well as their induced higher-body components to access their usefulness in *ab initio* nuclear structure calculations. We first note that in both cases, as the dimension of the P_{gen} model increases (i.e. as N_{gen} increases) there is less induced higher-body terms, but the energy only converges at a larger N_{max} . Thus using very large values of N_{gen} yields the same values as the bare interaction, while very small values of N_{gen} give results similar to using $G_s=T_{\text{rel}}$. This is clearly demonstrated in Fig. 6, where converged ${}^3\text{H}$ ground-state energies are shown for various N_{gen} values. Overall, the energies obtained for generator A and for generator B are somewhat similar to each other. Generator A consistently yields states that are slightly less bound than generator B which implies that less three-body forces are induced. This energy difference is more pronounced before convergence is achieved and also increases with N_{gen} before convergence. The converged values obtained for ${}^3\text{H}$ do not differ by much when using one generator or the other. Although the overall trends observed for ${}^4\text{He}$ are the same, since this nucleus is more tightly bound we observe firstly that the overall energies are greater and secondly that there is a larger difference between the converged energy given by the kinetic term and the ones from the bare interaction.

As already noted, the generators A and B that we introduced depend also on the HO frequency. In Fig. 7, we show the converged ${}^3\text{H}$ ground-state energies obtained with the generator B for a wide range of HO frequencies and N_{gen} values. In general, the bigger the $N_{\text{gen}}\hbar\Omega$ prod-

uct, the fewer NN repulsive short range correlations are transformed away by the SRG transformation, which in turn results in less binding of nuclei. The same trend is also observed for generator A in ${}^3\text{H}$ and ${}^4\text{He}$ calculations. The $G_s=T_{\text{rel}}$ and the bare interaction converged results are both frequency independent. Consequently the $G_s=T_{\text{rel}}$ SRG transformation is variational in HO frequency, while with generators A and B it is not.

Previous studies [20–23] analyzed the lambda dependence in the converged energy when using the kinetic term as the flow operator. They showed a significant λ dependence in calculations with NN -only interactions due to the fact that the low and the high momentum matrix elements are affected by the SRG transformation at different stages of the evolution because some of the information is transferred into $3N$ terms that were not taken into account. However this dependence was shown to be mostly removed when including the $3N$ interactions in the calculations, in particular when no initial chiral $3N$ interactions were included. In Figure 8, we examine the ${}^3\text{H}$ and ${}^4\text{He}$ ground-state energy variation as we evolve the Hamiltonians. The energies correspond to the converged values obtained for a given N_{gen} and a given HO frequency. Both generator A and generator B show basically no λ dependence for ${}^3\text{H}$ and very little such dependence in the case of ${}^4\text{He}$. This is contrary to the $G_s=T_{\text{rel}}$ case where, at first, the ground-state energy decreases as the repulsive short range part of the NN is transformed away and later it increases when the attractive part of the NN begins to be removed. The block generators that we introduced do not significantly affect the medium range attractive part of the NN potential and remove a smaller part of the short range repulsion. Consequently, the lambda dependence is much weaker and the binding energy larger.

We present a sample of our calculated ${}^3\text{H}$ and ${}^4\text{He}$ ground-state energies in Table I.

C. ${}^6\text{Li}$

We also performed similar calculations for the more complex nucleus ${}^6\text{Li}$. The NN interactions were SRG evolved in the HO Jacobi basis and then transformed into a HO Slater determinant (SD) basis used typically in all NCSM calculations with $A>4$. The SD basis simplifies the antisymmetrization of the wave function that becomes prohibitively difficult in Jacobi coordinates when using a larger number of nucleons, A.

We first consider the frequency dependence of the ${}^6\text{Li}$ ground-state energy when the $G_s=T_{\text{rel}}$ is used as the generator of the SRG transformation. These results are presented in Fig. 9. Since the use of a larger basis exponentially increases the computation time, we were generally limited to values of N_{max} up to 12 or 14. Note that even for the highest basis size, in this case $N_{\text{max}}=14$, the calculation has not yet fully converged but an accurate extrapolated value can be obtained, as described below.

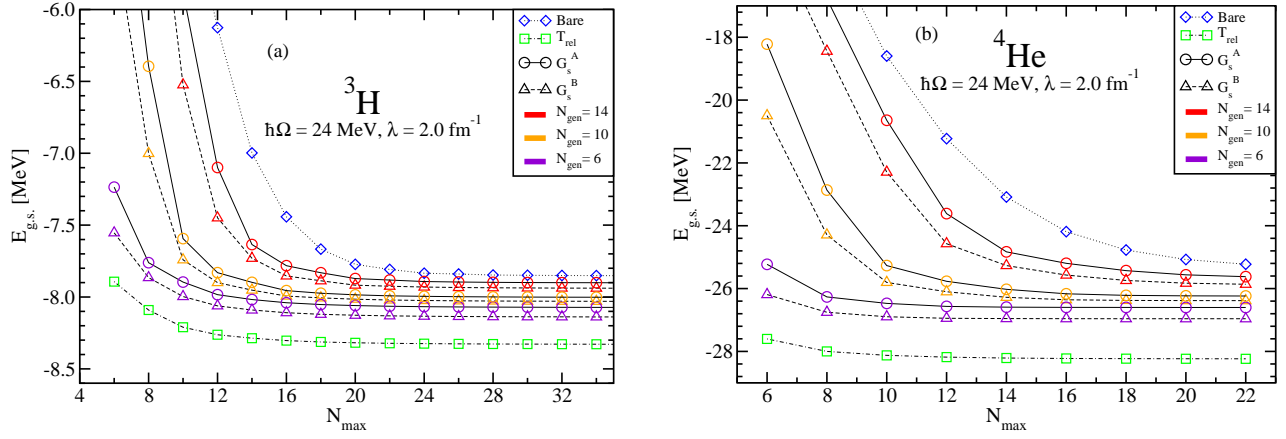


FIG. 5: (color online) Figure (a) shows the ground-state energy for ${}^3\text{H}$ as a function of N_{max} , for generators A and B at various N_{gen} , as well as for the bare initial interaction and for when the kinetic operator was used as the flow operator. The frequency is set to 24 MeV and λ is set to 2.0 fm^{-1} . (b) Same as above, but for ${}^4\text{He}$.

${}^3\text{H}$	$\lambda [\text{fm}^{-1}]$	N_{gen}	$\hbar\Omega [\text{MeV}]$	$E_{\text{g.s.}} [\text{MeV}]$	${}^4\text{He}$	$\lambda [\text{fm}^{-1}]$	N_{gen}	$\hbar\Omega [\text{MeV}]$	$E_{\text{g.s.}} [\text{MeV}]$
Bare	-	-	24	-7.85	Bare	-	-	24	-25.39
T_{rel}	2.0	-	24	-8.33	T_{rel}	2.0	-	24	-28.24
G_s^A	2.0	6	24	-8.07	G_s^A	2.0	6	24	-26.60
	2.0	10	24	-8.00		2.0	10	24	-26.24
	2.0	14	24	-7.90		2.0	14	24	-25.62
	2.0	18	24	-7.86		2.0	18	24	-25.29
	1.6	14	24	-7.90		1.6	14	24	-25.63
	1.2	14	24	-7.91		1.2	14	24	-25.64
	2.0	14	36	-7.81		2.0	14	36	-25.37
	2.0	14	16	-8.01		2.0	14	16	-26.23
G_s^B	2.0	6	24	-8.14	G_s^B	2.0	6	24	-26.96
	2.0	10	24	-8.03		2.0	10	24	-26.38
	2.0	14	24	-7.94		2.0	14	24	-25.86
	2.0	18	24	-7.87		2.0	18	24	-25.39
	1.6	14	24	-7.95		1.6	14	24	-25.91
	1.2	14	24	-7.95		1.2	14	24	-26.96
	2.0	14	36	-7.81		2.0	14	36	-25.37
	2.0	14	16	-8.04		2.0	14	16	-26.38

TABLE I: Ground-state energies of ${}^3\text{H}$ and ${}^4\text{He}$ for the different flow operators and various choices of parameters.

In this figure, we also observe a minimum in energy for each value of N_{max} although this minimum varies and tends towards smaller frequencies as N_{max} increases. Because the kinetic energy is frequency independent, the variational principle stipulates that the frequency with a minimum in energy should give the closest approximation of the true value. Moreover, since higher N_{max} values are closer to a converged value, we can adopt the frequency at the highest N_{max} as giving the best approximation, which in this case is 18 MeV.

We also obtained the ground-state energies for ${}^6\text{Li}$ for different sets of parameters using both generator A and

generator B. These generators are frequency dependent and thus the calculations are not variational in the HO frequency. However, minima in energy can still be found in most cases and we use the minimum of the highest N_{max} as our best approximation. An example is shown in Fig. 10 for $\lambda=2.0 \text{ fm}^{-1}$ and $N_{\text{gen}}=10$. Generators A and B give comparable results in this case although the use of the G_s^B flow operator results in somewhat lower energies and a flatter HO frequency dependence.

Nonetheless, like in most other cases, convergence was not yet achieved and thus we extrapolate to obtain converged energies. We fit the data using an exponential

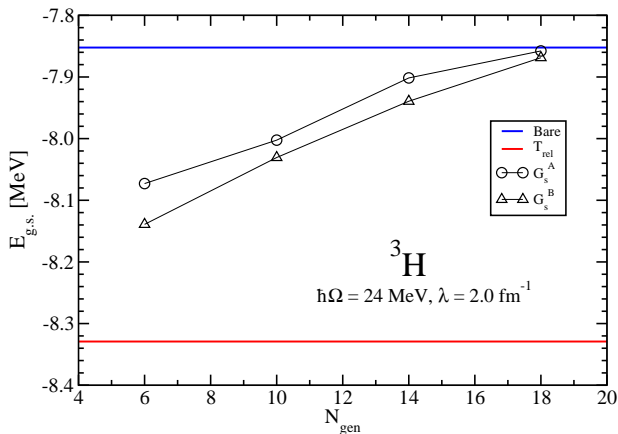


FIG. 6: (color online) Ground-state energy of ${}^3\text{H}$ as a function of N_{gen} with $\hbar\Omega=24$ MeV and $\lambda=2.0$ fm $^{-1}$. Results obtained with the bare initial NN potential and the SRG evolved with $G_s=T_{\text{rel}}$ are shown as full lines.

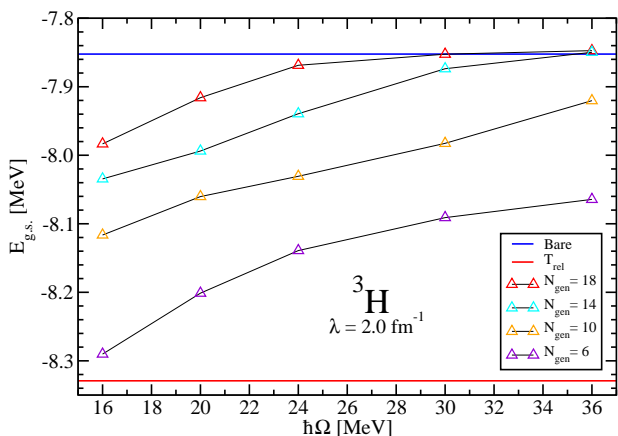


FIG. 7: (color online) Ground-state energy of ${}^3\text{H}$ as a function of HO frequency for different values of N_{gen} using G_s^B with $\lambda=2.0$ fm $^{-1}$.

ansatz

$$E_{\text{g.s.}} = E_0 + ae^{-bN_{\text{max}}}, \quad (8)$$

where a , b and E_0 are free parameters. E_0 is the extrapolated ground-state energy. We note that there exist more sophisticated extrapolation prescriptions [42–44], although they are typically applicable in the ultraviolet regime, i.e., in the high HO frequency region. Since we need an extrapolation at a fixed HO frequency that may not guarantee the ultraviolet convergence, we apply the above exponential ansatz applied in various studies in the past [45, 46].

However, the data does not strictly follow an exponential curve and therefore, the fit (8) provides a reasonable value when applied only to the data points corresponding to the larger values of N_{max} available. Figure 11 shows

Generator	λ [fm $^{-1}$]	N_{gen}	$\hbar\Omega$ [MeV]	$E_{\text{g.s.}}$ [MeV]
B	2.0	4	12	-32.82(6)
B	2.0	6	12	-32.41(7)
B	2.0	8	12	-31.8(1)
B	2.0	10	12	-31.2(2)
A	2.0	4	12	-32.6(1)
A	2.0	10	12	-30.7(3)
B	1.6	10	12	-31.6(1)
A	1.6	10	12	-31.0(2)
B	1.2	4	12	-33.98(2)
B	1.2	4	14	-34.06(2)
A	1.2	4	14	-34.54(1)
B	1.2	10	12	-31.90(8)
A	1.2	10	12	-31.2(2)
T_{rel}	2.0	-	18	-32.30(3)
Initial NN	-	-	-	-28.0(5)

TABLE II: Extrapolated ground-state energies of ${}^6\text{Li}$ in MeV with uncertainties in parentheses for the three generators and various choices of parameters. The initial NN value is based on results from Refs. [21, 22, 45].

	T_{rel}	G_s^A	G_s^B	Expt.
μ [μ_N]	0.848(1)	0.840(3)	0.841(2)	0.822
Q [e fm 2]	-0.053(18)	-0.054(30)	-0.049(29)	-0.082(2)
$B(M1; 0_1^+ 1 \rightarrow 1_1^+ 0)$	15.10(10)	14.91(5)	14.92(5)	15.43(32)
$B(M1; 2_1^+ 1 \rightarrow 1_1^+ 0)$	0.024(4)	0.024(2)	0.025(2)	0.149(27)
$E_{\text{g.s.}}$ [MeV]	-32.30(3)	-30.7(3)	-31.2(2)	-31.995

TABLE III: Magnetic moment, quadrupole moment, B(M1) transition probabilities (in μ_N^2) and extrapolated ground-state energies of ${}^6\text{Li}$ for different flow operators when $\lambda=2.0$ fm $^{-1}$, $N_{\text{gen}}=10$, and $\hbar\Omega=12$ MeV. Experimental values are taken from [47].

an example of fitted exponential curves to two data sets where $\hbar\Omega=12$ MeV, $\lambda=2.0$ fm $^{-1}$ and $N_{\text{gen}}=10$ or $N_{\text{gen}}=4$. The sample of extrapolated values, presented in Table II was obtained from a three-points fit at the selected HO frequency, $\hbar\Omega$. The uncertainty is taken from variations of the number of extrapolated points. We also compare to the extrapolated calculation with $G_s=T_{\text{rel}}$, and, further, to the initial NN potential result based on SRG calculations of Refs. [21, 22] with the $3N$ -induced interactions included and on the Okubo-Lee-Suzuki calculations of Ref. [45].

Overall, the trends are similar to those observed in ${}^3\text{H}$ and ${}^4\text{He}$ calculations. A larger block model space P_{gen} (higher N_{gen}) results in binding energies closer to that of the initial interaction, a lower N_{gen} then takes us closer

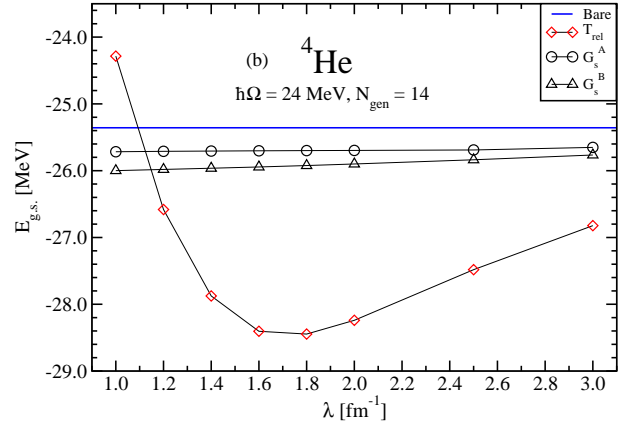
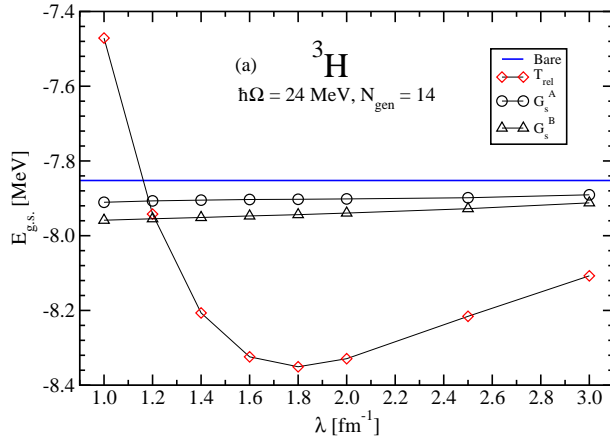


FIG. 8: (color online) Ground-state energy of ${}^3\text{H}$ (a) and ${}^4\text{He}$ (b) as a function of the flow parameter for the three different generators as well as the ground-state energy obtained using the bare initial interaction. For generators A and B, $N_{\text{gen}}=14$ and the HO frequency of $\hbar\Omega=24$ MeV was used. All energy values are converged or extrapolated.

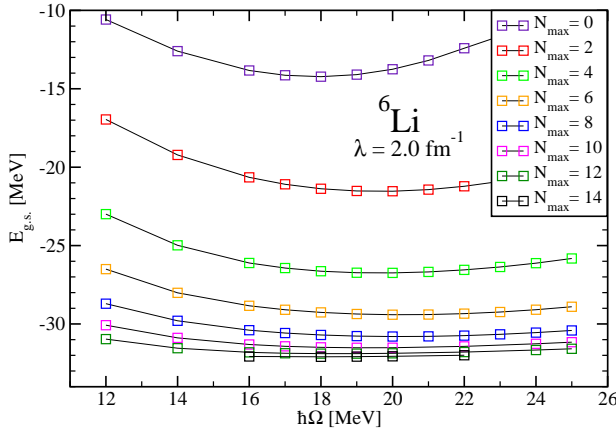


FIG. 9: (color online) Ground-state energy as a function of HO frequency using the $G_s=T_{\text{rel}}$ flow operator for different values of N_{max} with $\lambda=2.0$ fm $^{-1}$.

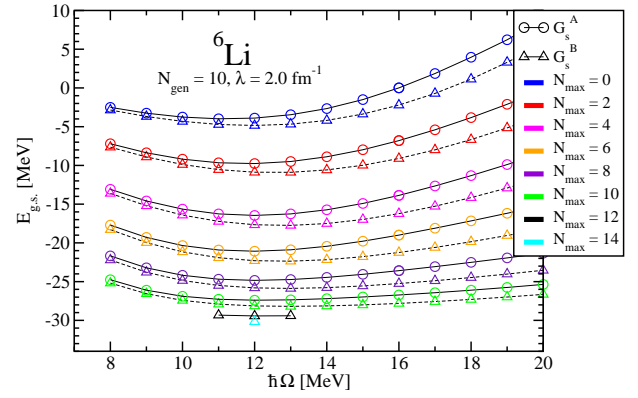


FIG. 10: (color online) Ground-state energy as a function of HO frequency using generator A and B for different values of N_{max} with $\lambda=2.0$ fm $^{-1}$ and $N_{\text{gen}}=10$.

to calculations with the $G_s=T_{\text{rel}}$ flow operator. This is also illustrated in Fig. 12.

Calculations discussed so far suggest that the performance of the generators A and B is very similar with the generator A giving somewhat higher binding energies while the convergence is slightly faster with the generator B. However, we observe significant differences in ${}^6\text{Li}$ calculations with these two generators at larger N_{max} values when using a small value of N_{gen} ($N_{\text{max}} \gg N_{\text{gen}}$) combined with a smaller lambda. This is illustrated in Fig. 13, where we present ${}^6\text{Li}$ ground-state energies for both generators using $N_{\text{gen}}=4$ and $\lambda=1.2$ fm $^{-1}$ for different basis sizes and a wide range of HO frequencies. While the results obtained with the generator B are similar to those found with higher λ and N_{gen} (compare Fig. 10), when generator A is used we observe minima at $N_{\text{max}}=0$ and $N_{\text{max}}=2$ that shift fast to the right towards higher

HO frequencies with increasing N_{max} . For larger values of N_{max} we do not find a minimum in energy in the frequency range up to 22 MeV displayed in the figure. At the same time, we find a dramatic increase of the binding energy with increasing $\hbar\Omega$. In fact the binding energy becomes much larger than that obtained with the standard $G_s=T_{\text{rel}}$ generator. We believe this to be due to the structural nature of the generator A. Indeed, when using a basis space N_{max} with a dimension larger than the P_{gen} block generator size characterized by the N_{gen} , we probe evolved NN matrix elements in the Q_{gen} space. The strong coupling at the boundary of the P_{gen} and Q_{gen} spaces, due to the kinetic operator, induces significant off-diagonal matrix elements beyond the P_{gen} space when the NN potential is evolved to a small λ (see Fig. 2), which most likely contributes to the increase in binding. As demonstrated in Sect. III A, the generator B does not induce such off-diagonal matrix elements.

Finally, we analyzed the lambda dependence of the ${}^6\text{Li}$

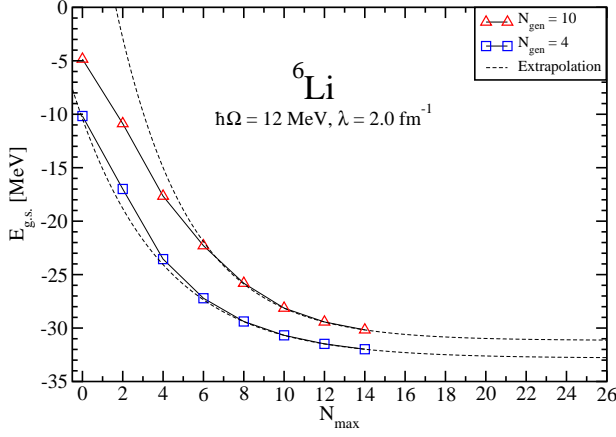


FIG. 11: (color online) Ground-state energy as a function of N_{\max} for generator B using $\lambda=2.0 \text{ fm}^{-1}$ and $N_{\text{gen}}=10$. Results are shown for the minimum frequency of 12 MeV associated with this specific set of parameters. The extrapolated curve is also shown.

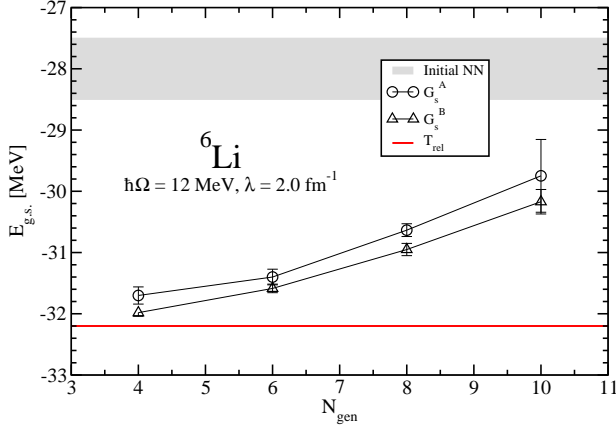


FIG. 12: (color online) Ground-state energy as a function of N_{gen} for G_s^A and G_s^B with $\hbar\Omega=12 \text{ MeV}$ and $\lambda=2.0 \text{ fm}^{-1}$. The result obtained with the $G_s=T_{\text{rel}}$ is shown by the solid line. The shaded band represents the initial NN value with its uncertainty based on results from Refs. [21, 22, 45].

results. Figure 14 shows the extrapolated ${}^6\text{Li}$ ground-state energies as a function of λ when using generators A and B with different values of N_{gen} and a fixed $\hbar\Omega=12 \text{ MeV}$. It is well known that there is a significant λ dependence when using the $G_s=T_{\text{rel}}$ generator in NN -only calculations [21, 22]. Using generator A or B does not remove this dependence although it is greatly minimized. We observe that using larger values of λ and, in particular, larger values of N_{gen} yields results that are closer to the initial NN interaction value, i.e., the included many-body interactions are less significant.

So far we have discussed only ground-state energy re-

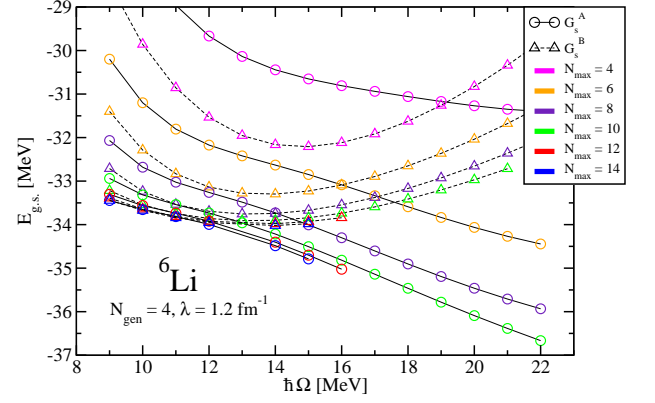


FIG. 13: (color online) Ground-state energy as a function of HO frequency using generators A and B for different values of N_{\max} with $\lambda=1.2 \text{ fm}^{-1}$ and $N_{\text{gen}}=4$.

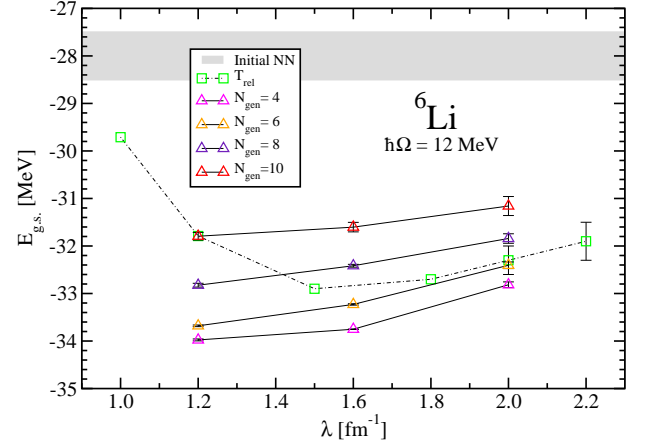


FIG. 14: (color online) Ground-state energy as a function of λ using generators A and B for a range of N_{gen} values and $\hbar\Omega=12 \text{ MeV}$. Results obtained with the $G_s=T_{\text{rel}}$ (connected by the dotted line) are independent of the HO frequency. The shaded band represents the initial NN value with its uncertainty based on results from Refs. [21, 22, 45].

sults. In Fig. 15 we compare ${}^6\text{Li}$ excitation energies obtained with the generators A, B and the standard $G_s=T_{\text{rel}}$ to experiment. We use the values of $N_{\text{gen}}=10$ and $\lambda=2.0 \text{ fm}^{-1}$, best performing in the ground-state calculations (Fig. 14). We find that all the SRG generators give similar excitation spectra that are in a reasonable agreement with experiment. We note that only the ground state of ${}^6\text{Li}$ is bound, the excited states are resonances above the ${}^4\text{He}+d$ threshold. However, the 3^+ and the 0^+ states are very narrow, therefore we can be confident that our NCSM HO basis calculations are capable of describing these states well. That is not true for the broad 2^+ and 1^+ d - ${}^4\text{He}$ D -wave resonances. In Table III, we present the ground-state mag-

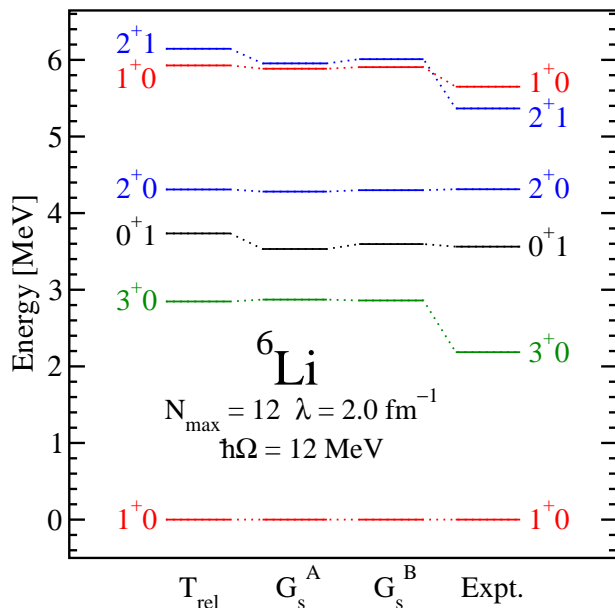


FIG. 15: (color online) Excited states of ${}^6\text{Li}$ in MeV obtained with $G_s=T_{\text{rel}}$, G_s^A , and G_s^B . Experimental data from [47] are also shown.

netic and quadrupole moments, and selected B(M1) transition probabilities calculated with the three respective generators. As for the excitation energies, the differences are minimal and the agreement with experiment is quite satisfactory.

IV. CONCLUSIONS AND OUTLOOK

We evolved the chiral NN interaction by SRG transformations using two novel generators with flow operators G_s of block structure in the HO basis. The first generator (A), see Eq. (5), was motivated by an OLS-type decoupling of the model space P_{gen} , defined by a HO cut $N \leq N_{\text{gen}}$, and the $Q_{\text{gen}}=1-P_{\text{gen}}$ space. The second one (B), see Eq. (6), was constructed in a way that would leave invariant a Hamiltonian consisting of a kinetic energy plus a NN potential with negligible matrix elements for basis states with $N > N_{\text{gen}}$. We found that both generators drive the two-body Hamiltonians to block diagonal structure. The evolved NN potentials were then used in NCSM calculations for ${}^3\text{H}$, ${}^4\text{He}$ and ${}^6\text{Li}$. We varied the SRG evolution parameter s as well as the cut N_{gen} and compared binding energy results to calculations with the standard generator, $G_s=T_{\text{rel}}$, as well as to the exact binding energies obtained with the initial chiral NN potential.

We observed that a good convergence comparable to that of the standard $G_s=T_{\text{rel}}$ generator can be achieved with both block generators if N_{gen} is chosen lower than a reachable N_{max} of the many-nucleon basis. We also observed that unless the N_{gen} is too small (i.e., $\lesssim 6$), the block generators appear to induce weaker many-body forces than the standard $G_s=T_{\text{rel}}$ generator, i.e., the calculated binding energies are closer to the exact ones when using the block generators. Further, the dependence on the flow parameter s appears weaker and more monotonic with the block generators.

When comparing the performance of the two block generators, we saw in ${}^6\text{Li}$ calculations that with the first one (A) the HO frequency dependence becomes stronger and at high frequencies the induced many-body forces become significant. This is most likely related to the fact that at large $N_{\text{max}} \gg N_{\text{gen}}$ the Q -space part of the NN potential is probed and, further, that the strong coupling at the boundary of the P_{gen} and Q_{gen} spaces due to the kinetic operator, induces significant off-diagonal matrix elements beyond the P_{gen} space.

Overall, by using the generator (B) with a selected sufficiently large N_{gen} related to the highest reachable N_{max} by $N_{\text{gen}} \sim N_{\text{max}} - 4$, and, further, by selecting a sufficiently small s so that the convergence of the many-nucleon calculation can still be reached, we can minimize the induced many-body force and obtain results closer to the exact ones compared to calculations with the standard $G_s=T_{\text{rel}}$ generator.

Obviously, the next task is to test the block generators in three-body space also including initial chiral $3N$ interactions and study if the problem of the induced $4N$ interaction will be alleviated. An important issue to explore is the embedding of the evolved two- and three-body interactions in many-body spaces. Also, one may want to test analogous block generators defined in the momentum space rather than in the HO basis as done in this work. A separate important problem to be explored is the evolution of general operators [40, 41].

Acknowledgments

Computing support for this work came in part from the LLNL institutional Computing Grand Challenge program and from an INCITE Award on the Titan supercomputer of the Oak Ridge Leadership Computing Facility (OLCF) at ORNL. Support from the Natural Sciences and Engineering Research Council of Canada (NSERC) Grant No. 401945-2011. TRIUMF receives funding via a contribution through the National Research Council Canada.

[1] E. Epelbaum, H.-W. Hammer, and U.-G. Meiner, Rev. Mod. Phys. 81, 1773 (2009).

[2] R. Machleidt and D. R. Entem, Phys. Rept. 503, 1

- (2011).
- [3] P. Navrátil, J. P. Vary and B. R. Barrett, *Phys. Rev. Lett.* **84**, 5728 (2000).
- [4] B. R. Barrett, P. Navrátil and J. P. Vary, *Prog. Part. Nucl. Phys.* **69**, 131 (2013).
- [5] G. Hagen, T. Papenbrock, M. Hjorth-Jensen and D. J. Dean, arXiv:1312.7872 [nucl-th].
- [6] S. Binder, J. Langhammer, A. Calci, P. Navrátil and R. Roth, *Phys. Rev. C* **87**, 021303 (2013).
- [7] A. Cipollone, C. Barbieri and P. Navrátil, *Phys. Rev. Lett.* **111**, 062501 (2013).
- [8] H. Hergert, S. Binder, A. Calci, J. Langhammer and R. Roth, *Phys. Rev. Lett.* **110**, no. 24, 242501 (2013).
- [9] S. Baroni, P. Navrátil and S. Quaglioni, *Phys. Rev. Lett.* **110**, 022505 (2013).
- [10] S. Baroni, P. Navrátil and S. Quaglioni, *Phys. Rev. C* **87**, no. 3, 034326 (2013).
- [11] G. Hagen and N. Michel, *Phys. Rev. C* **86**, 021602 (2012).
- [12] G. Hagen, M. Hjorth-Jensen, G. R. Jansen, R. Machleidt and T. Papenbrock, *Phys. Rev. Lett.* **109**, 032502 (2012).
- [13] A. Ekström, G. Baardsen, C. Forssén, G. Hagen, M. Hjorth-Jensen, G. R. Jansen, R. Machleidt and W. Nazarewicz *et al.*, *Phys. Rev. Lett.* **110**, 192502 (2013).
- [14] S. D. Glazek and K. G. Wilson, *Phys. Rev. D* **48**, 5863 (1993); **49**, 4214 (1994).
- [15] F. Wegner, *Ann. de Phys.* **506**, 77 (1994); *Phys. Rep.* **348**, 77 (2001).
- [16] R. J. Furnstahl, *Nucl. Phys. Proc. Suppl.* **228**, 139 (2012).
- [17] R. J. Furnstahl and K. Hebeler, *Rept. Prog. Phys.* **76**, 126301 (2013).
- [18] S. K. Bogner, R. J. Furnstahl and R. J. Perry, *Phys. Rev. C* **75**, 061001 (2007).
- [19] S. Kehrein, *Springer Tracts Mod. Phys.* **217**, 137 (2006).
- [20] E. D. Jurgenson, P. Navrátil and R. J. Furnstahl, *Phys. Rev. Lett.* **103**, 082501 (2009).
- [21] E. D. Jurgenson, P. Navrátil and R. J. Furnstahl, *Phys. Rev. C* **83**, 034301 (2011).
- [22] R. Roth, J. Langhammer, A. Calci, S. Binder and P. Navrátil, *Phys. Rev. Lett.* **107**, 072501 (2011).
- [23] R. Roth, S. Binder, K. Vobig, A. Calci, J. Langhammer and P. Navrátil, *Phys. Rev. Lett.* **109**, 052501 (2012).
- [24] D. R. Entem and R. Machleidt, *Phys. Rev. C* **68**, 041001 (2003).
- [25] R. Roth, private communication.
- [26] R. Roth, T. Neff and H. Feldmeier, *Prog. Part. Nucl. Phys.* **65**, 50 (2010).
- [27] K. Hebeler, *Phys. Rev. C* **85**, 021002 (2012).
- [28] K. A. Wendt, *Phys. Rev. C* **87**, no. 6, 061001 (2013).
- [29] K. A. Wendt, R. J. Furnstahl and R. J. Perry, *Phys. Rev. C* **83**, 034005 (2011).
- [30] E. Anderson, S. K. Bogner, R. J. Furnstahl, E. D. Jurgenson, R. J. Perry and A. Schwenk, *Phys. Rev. C* **77**, 037001 (2008).
- [31] S. Bogner, T. T. S. Kuo, L. Coraggio, A. Covello and N. Itaco, *Phys. Rev. C* **65**, 051301 (2002).
- [32] S. K. Bogner, T. T. S. Kuo and A. Schwenk, *Phys. Rept.* **386**, 1 (2003).
- [33] W. Li, E. R. Anderson and R. J. Furnstahl, *Phys. Rev. C* **84**, 054002 (2011).
- [34] S. Okubo, *Prog. Theor. Phys.* **12**, 603 (1954).
- [35] K. Suzuki and S. Y. Lee, *Prog. Theor. Phys.* **64**, 2091 (1980).
- [36] Suzuki K 1982 *Prog. Theor. Phys.* **68** 246.
- [37] Suzuki K and Okamoto R 1983 *Prog. Theor. Phys.* **70** 439.
- [38] A. M. Shirokov, A. I. Mazur, S. A. Zaytsev, J. P. Vary and T. A. Weber, *Phys. Rev. C* **70**, 044005 (2004)
- [39] P. Navrátil, G. P. Kamuntavicius and B. R. Barrett, *Phys. Rev. C* **61**, 044001 (2000).
- [40] E. R. Anderson, S. K. Bogner, R. J. Furnstahl and R. J. Perry, *Phys. Rev. C* **82**, 054001 (2010).
- [41] M. D. Schuster, S. Quaglioni, C. W. Johnson, E. D. Jurgenson and P. Navrátil, arXiv:1402.7106 [nucl-th].
- [42] S. A. Coon, M. I. Avetian, M. K. G. Kruse, B. van Kolck, P. Maris and J. P. Vary, *Phys. Rev. C* ,
- [43] R. J. Furnstahl, G. Hagen and T. Papenbrock, *Phys. Rev. C* **86**, 031301 (2012) [arXiv:1207.6100 [nucl-th]].
- [44] S. More, A. Ekström, R. J. Furnstahl, G. Hagen, and T. Papenbrock, *Phys. Rev. C* **87**, 044326 (2013).
- [45] P. Navrátil and E. Caurier, *Phys. Rev. C* **69**, 014311(2004).
- [46] S. K. Bogner, R. J. Furnstahl, P. Maris, R. J. Perry, A. Schwenk, and J. P. Vary, *Nucl. Phys. A* **801**, 21 (2008).
- [47] D. R. Tilley, C. M. Cheves, J. L. Godwin, G. M. Hale, H. M. Hofmann, J.H. Kelley, C.G. Sheu, H.R. Weller, *Nuclear Physics A* **708**, 3 (2002).